

Rethinking the Stability-Plasticity Trade-off in Continual Learning from an Architectural Perspective

Aojun Lu¹ Hangjie Yuan² Tao Feng³ Yanan Sun¹

Abstract

The quest for Continual Learning (CL) seeks to empower neural networks with the ability to learn and adapt incrementally. Central to this pursuit is addressing the stability-plasticity dilemma, which involves striking a balance between two conflicting objectives: preserving previously learned knowledge and acquiring new knowledge. While numerous CL methods aim to achieve this trade-off, they often overlook the impact of network architecture on stability and plasticity, restricting the trade-off to the parameter level. In this paper, we delve into the conflict between stability and plasticity at the architectural level. We reveal that under an equal parameter constraint, deeper networks exhibit better plasticity, while wider networks are characterized by superior stability. To address this architectural-level dilemma, we introduce a novel framework denoted Dual-Arch, which serves as a plug-in component for CL. This framework leverages the complementary strengths of two distinct and independent networks: one dedicated to plasticity and the other to stability. Each network is designed with a specialized and lightweight architecture, tailored to its respective objective. Extensive experiments demonstrate that Dual-Arch enhances the performance of existing CL methods while being up to **87%** more compact in terms of parameters.

challenge in CL is catastrophic forgetting (McCloskey & Cohen, 1989; Goodfellow et al., 2013), i.e., directly updating neural networks to learn new data causes rapid forgetting of previously acquired knowledge. To learn continually without forgetting, a neural network must balance plasticity, to learn new concepts, and stability, to retain acquired knowledge. However, emphasizing stability can limit the neural network’s ability to acquire new knowledge, while excessive plasticity can lead to severe forgetting, a challenge known as the stability-plasticity dilemma (Grossberg, 2013).

To enhance CL, most of the research efforts (Li & Hoiem, 2017; Henning et al., 2021; Feng et al., 2022) are centered on developing novel learning methods that achieve a better trade-off between stability and plasticity. These methods involve adding loss terms that prevent the model from changing, replaying past data, or explicitly using distinct parts of the network for different tasks, *etc* (Wang et al., 2024a). In particular, architecture-based methods have achieved great success across various CL scenarios (Rusu et al., 2016; Rosenfeld & Tsotsos, 2018; Wang et al., 2023). Characteristically, this type of method introduces an extra part of the network that is solely trained on the current data, which is then integrated with other parts that have been continuously trained on the previous data (Yan et al., 2021; Zhou et al., 2023b). Since a new independent parameter space is used to learn the current data, these methods avoid rewriting the original parameters, thus preserving the old knowledge. In this way, the conflict between stability and plasticity at the parameter level can be significantly mitigated.

While studies that focus on expanding and allocating architecture have achieved notable success, research on the basic architectures for CL is still in its infancy. This gap is crucial because, despite the ability of advanced learning methods to optimize parameters effectively, the overall CL performance remains constrained by suboptimal architectures (Lu et al., 2024). In this regard, certain pioneer works have concluded that wider and shallower networks exhibit superior overall CL performance, mainly contributing to enhanced stability (Mirzadeh et al., 2022a;b). However, theoretical analyses and practices (Simonyan & Zisserman, 2014; He et al., 2016; Liang & Srikant, 2017; Raghu et al., 2017; Zhao et al., 2024) have demonstrated that deeper networks pos-

1. Introduction

Continual Learning (CL) seeks to enable neural networks to continuously acquire and update knowledge. The primary

¹College of Computer Science, Sichuan University, Chengdu, China ²College of Computer Science and Technology, Zhejiang University, Hangzhou, China ³Department of Computer Science and Technology, Tsinghua University, Beijing, China. Correspondence to: Tao Feng <fengtao.hi@gmail.com>.

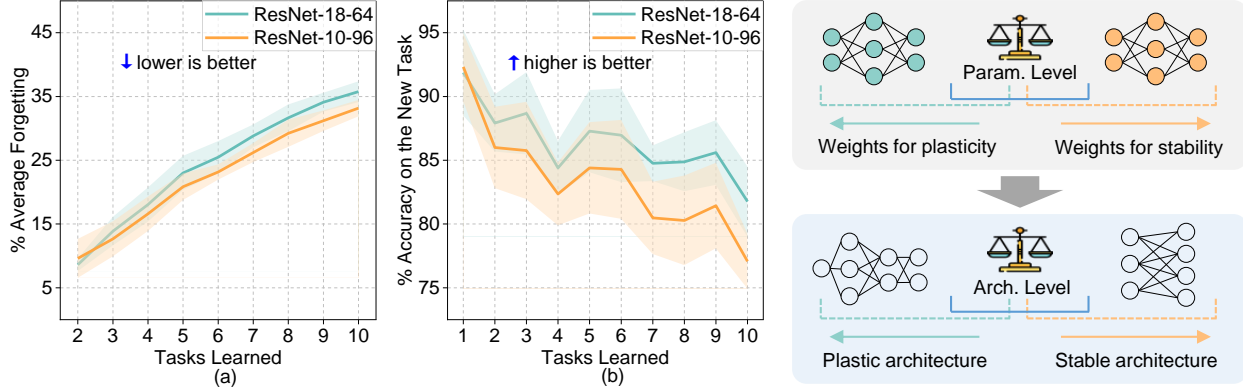


Figure 1: **Left.** (a) The average forgetting and (b) the accuracy on the new task of ResNet-18 and its wider and shallower variant. Details are presented in Sec. 3. **Right.** While existing research mainly optimizes weights (represented by node colors) for the stability-plasticity trade-off at the parameter level, this study proposes a novel insight for extending this trade-off to the architectural level.

sess enhanced representation learning ability, indicating the important role of depth in facilitating plasticity. These findings raise a concern regarding whether there is an inherent conflict between stability and plasticity at the architectural level under a given parameter count constraint.

To investigate this, we conducted a comparison between ResNet-18 (He et al., 2016) and its wider yet shallower variant, evaluating their average forgetting and accuracy on the new task. As shown in Fig. 1, ResNet-18 achieves higher accuracy on the new task, indicative of better plasticity, whereas the wider yet shallower variant exhibits lower average forgetting, indicative of greater stability. However, both networks underperform in the other aspect, which indicates there may exist a stability-plasticity dilemma at the architectural level as well. Given that existing works (Zhou et al., 2023b; Lu et al., 2024) typically employ a uniform architecture for both stability and plasticity, this inherent dilemma may limit CL performance, even when the architecture and parameters are finely optimized.

How to balance the stability and plasticity at the architectural level? An intuitive and straightforward solution is to combine two independent models with distinct architectures: one dedicated to plasticity and the other to stability. Previous studies on CL have demonstrated that incorporating an auxiliary model, specifically trained on the current data, can enhance the plasticity of the primary model (Kim et al., 2023; Bonato et al., 2024). Building on these insights, we extend from an architectural perspective, proposing a novel framework that employs a plastic architecture to acquire new knowledge, which is then transferred to the main model with a stable architecture. Specifically, knowledge distillation (Hinton et al., 2015; Romero et al., 2014) is utilized for this transfer due to its proven efficacy in transferring knowledge between networks with different archi-

tectures (Gou et al., 2021). Consequently, our proposed framework, **Dual-Architecture** (Dual-Arch), leverages the complementary strengths of two distinct architectures, effectively balancing stability and plasticity at the architectural level. Extensive experiments show that Dual-Arch markedly enhances CL performance with significantly fewer parameters when compared to the baselines. Code is available at <https://github.com/byyx666/Dual-Arch>.

The contributions of this study are outlined as follows:

- We empirically demonstrate that existing architectural designs typically exhibit good plasticity but poor stability, while their wider and shallower variants exhibit the opposite traits. Based on these findings, we propose a novel insight for exploring the stability-plasticity trade-off from an architectural perspective.
- We introduce a novel CL framework, Dual-Arch, which employs dual architectures dedicated to stability and plasticity and thus combines both advantages. Furthermore, Dual-Arch can be naturally incorporated with various CL methods as a plug-and-play component.
- Extensive experiments demonstrate that Dual-Arch is parameter-efficient, i.e., attaining better performance with a remarkably reduced parameter count than using a single architecture.

2. Related Work

CL involves letting models sequentially learn a series of tasks without or with limited access to previous tasks. Based on whether the task identity is provided or must be inferred, CL can be broadly categorized into three typical scenarios: Task/Class/Domain Incremental Learning (IL) (Van de Ven et al., 2022). This study mainly focuses on the most general and realistic scenario of these three, i.e., *Class IL*, where the

task identity is unknown during inference (Van de Ven et al., 2022; Wang et al., 2024a).

2.1. Learning Methods for CL

To address catastrophic forgetting, the CL community has developed a variety of learning methods aimed at striking a balance between stability and plasticity (Feng et al., 2025). These methods can be broadly categorized into three main approaches: replay-based methods, regularization-based methods, and architecture-based methods. **Replay-based methods** keep a subset of the previous data information in a memory buffer, which is subsequently exploited to approximate old data distributions during training (Aljundi et al., 2019; Iscen et al., 2020; Qin et al., 2023). A common and effective implementation involves jointly training the model on both the stored data and the current task data (Robins, 1995; Chaudhry et al., 2018). It is important to note that replay-based methods are often combined with other techniques to enhance their effectiveness (Rebuffi et al., 2017; Yan et al., 2021). **Regularization-based methods** introduce a regularization loss term to balance the learning of new tasks with the retention of old tasks. These methods can be further divided into two subcategories based on the target of regularization (Wang et al., 2024a). The first is *weight regularization*, which selectively constrains the variation of the network parameters based on their importance to previously learned tasks, e.g., EWC (Kirkpatrick et al., 2017) and SI (Zenke et al., 2017). The second is *function regularization* (Bian et al., 2024), which employs techniques such as knowledge distillation (Romero et al., 2014) to maintain consistency between the outputs of the original and updated models, e.g., iCaRL (Rebuffi et al., 2017) and WA (Zhao et al., 2020). **Architecture-based methods** dynamically allocate task-specific network parameter space for each task to mitigate inter-task interference, thereby balancing stability and plasticity (Yoon et al., 2017). These methods typically involve dynamically expanding the networks, such as DER (Yan et al., 2021) and MEMO (Zhou et al., 2023b).

Discussion. In principle, the performance of neural networks is jointly influenced by their parameters and architectures. While the learning methods mentioned above mainly enhance CL by optimizing the parameters or extending parameter space, the suboptimal basic architectures might still limit CL performance. Our study aims to address this by proposing a plug-and-play framework that leverages the complementary strengths of two distinct architectures.

2.2. Neural Architectures for CL

Besides learning methods, there is a body of research (Mirzadeh et al., 2022a;b; Pham et al., 2022) that concentrates on exploring optimal neural architectures for CL. In particular, ArchCraft (Lu et al., 2024) delves into

the influence of various network components and scaling on CL performance, demonstrating that certain architectural designs are more CL-friendly than existing ones. Furthermore, it is shown that a well-designed architecture can achieve superior CL performance with a smaller parameter count, which is particularly beneficial for memory-constrained environments (Lu et al., 2024). These studies emphasize that the impact of architectural designs on CL performance is at least as significant as that of the learning methods. However, it should be noted that existing studies focus exclusively on the impact of architectures on the overall performance of CL. Our work extends this line of inquiry by highlighting the inherent conflict between stability and plasticity at the architectural level and subsequently proposing a novel solution to address it.

2.3. Multi Models for CL

Various existing studies have proposed employing additional models to enhance CL (Li & Hoiem, 2017; Kim et al., 2023; Bonato et al., 2024). In particular, certain works (Pham et al., 2021; Arani et al., 2022) based on complementary learning systems (McClelland et al., 1995; Kumaran et al., 2016) utilize two learners (known as slow and fast learners) with different functions to achieve CL. Among them, MKD (Michel et al., 2024) and Hare & Tortoise (Lee et al., 2024) employ techniques such as exponential moving averages to integrate knowledge across two models, effectively balancing stability and plasticity. Our proposed solution shares a similar conceptual framework, crafting two independent learners that assume roles of plasticity and stability respectively during the CL process. However, unlike these prior efforts that employ a uniform architecture for all models, our study emphasizes the importance of specific architectural designs tailored to each learner. By doing so, our study provides novel insights into more effectively leveraging multiple models for CL.

3. Architectural Dimensions of Stability and Plasticity

This section presents an investigation of the impact of architectural designs on the stability and plasticity of neural networks. The primary objective of this investigation is to reveal the conflict between stability and plasticity at the architectural level, with a focus on network scaling.

3.1. Empirical Study Settings

Architectural Variants. ResNet-18 (He et al., 2016) is selected as the foundational architecture, given its extensive utilization in existing CL research (Yan et al., 2021; Goswami et al., 2024). Our primary focus is on examining the impact of depth and width on CL. To this end, we vary

Table 1: The performance (%) of the original ResNet-18 (gray background) and its variants. We report the mean and std of 5 runs with different task orders. Note that the ‘#P’ denotes the parameter counts of a single architecture here.

Depth	Width	Penultimate Layer	#P (M)	AAN \uparrow	FAF \downarrow	FRF \downarrow
18	64	GAP	11.23	86.41 \pm 0.60	35.76 \pm 1.62	41.09 \pm 2.08
10	96	GAP	11.10	83.44 \pm 0.84 (-2.97)	33.16 \pm 1.28 (-2.60)	39.15 \pm 2.06 (-1.94)
18	64	4 \times 4 AvgPool	11.38	84.64 \pm 0.43 (-1.77)	34.17 \pm 2.03 (-1.59)	39.97 \pm 2.71 (-1.12)
26	52	GAP	11.56	86.68 \pm 0.70 (+0.27)	36.02 \pm 1.79 (+0.26)	41.20 \pm 2.37 (+0.11)

the number of layers and initial channel counts in ResNet-18 while maintaining a relatively constant total parameter count. Additionally, we conduct an extended study to investigate the effect of pre-classification width. This involves replacing the global average pooling (GAP) layer with a 4×4 average pooling layer with a stride of 3, thereby producing an output feature map of size 2×2 .

Implementation Setup. A subset of ImageNet (Deng et al., 2009), known as ImageNet100 (Rebuffi et al., 2017), is utilized as the dataset. It is partitioned into 10 incremental tasks, each comprising 10 classes. All models are trained using iCaRL (Rebuffi et al., 2017), a classic learning method in the CL field, with a fixed memory size of 2,000 exemplars.

Evaluation Metrics.

To evaluate plasticity, we measure the Average Accuracy on New tasks (AAN) across all incremental steps, where higher values indicate greater plasticity. For stability assessment, we employ two complementary metrics: Average Forgetting (AF) and Relative Forgetting (RF). AF measures the absolute stability after learning the k -th task, calculated as $AF_k = \frac{1}{k-1} \sum_{b=1}^{k-1} (a_b^* - a_b)$, where a_b denotes the current accuracy on task b and a_b^* represents its peak past accuracy. RF (Wang et al., 2024b) provides a normalized stability measure to avoid penalizing highly plastic models, defined as $RF = \frac{1}{k-1} \sum_{b=1}^{k-1} (1 - \frac{a_b}{a_b^*})$. We specifically use the final-task values (FAF and FRF) as overall stability indicators, with lower values corresponding to better stability.

3.2. Empirical Study Results

The performance comparison between ResNet-18 and its variants, under comparable parameter counts (within $\pm 3\%$ margin), is summarized in Tab. 1. We observe that making the network shallower but wider decreases both AAN and forgetting metrics (FAF and FRF), indicating enhanced stability but reduced plasticity. This trend similarly emerges when increasing the pre-classification width through penultimate layer modification, further confirming that wider architectures improve stability while compromising plasticity. Conversely, a deeper yet narrower variant exhibits a slight increase in both AAN and forgetting measures, suggesting

marginally improved plasticity with reduced stability. These results reveal an inherent trade-off between stability and plasticity at the architectural level, governed by architectural design choices within specific parameter limits.

4. Dual-Architecture for CL

In this section, we propose Dual-Arch, a framework that can be easily plugged in existing CL methods, to address the stability-plasticity dilemma at the architectural level. Specifically, we will provide an overview of the Dual-Arch framework and detail its learning algorithm.

4.1. Preliminaries

Before further description, some definitions related to the CL are presented. CL aims to learn from a dynamic data stream. Following convention (Zhou et al., 2023a), we consider a sequence of K tasks (also known as steps) $\{\mathcal{D}_1, \mathcal{D}_2, \dots, \mathcal{D}_K\}$ without overlapping classes. Specifically, $\mathcal{D}_k \sim \{\mathcal{X}_k, \mathcal{Y}_k\}$ represents the data of the k -th step, containing N_k classes. Here, \mathcal{X}_k denotes the set of samples, and \mathcal{Y}_k denotes their respective labels. At the k -th step, the CL model is trained on \mathcal{D}_k^{train} and then tested on $\mathcal{D}_{0:k}^{test}$, which denotes the joint test dataset from task 0 to task k . For replay-based methods, parts of data from previous tasks are preserved and incorporated into the \mathcal{D}_k^{train} .

In the traditional CL paradigm using a single learner, the training loss at the k -th step can be formulated as:

$$L_{single} = L_{CE} + L_{CL}, \quad (1)$$

where the loss term L_{CE} is the classification loss calculated using a cross-entropy loss function, and L_{CL} is specifically defined by the particular used CL methods. Specifically, we consider the CL learner parameterized by weights θ_k and we use $o(x)$ to indicate the output logits of the learner on input x . the L_{CE} is defined as:

$$L_{CE}(x, y; \theta_k) = -\log \frac{\exp(o_y)}{\sum_{m=1}^{N_k} \exp(o_m)}. \quad (2)$$

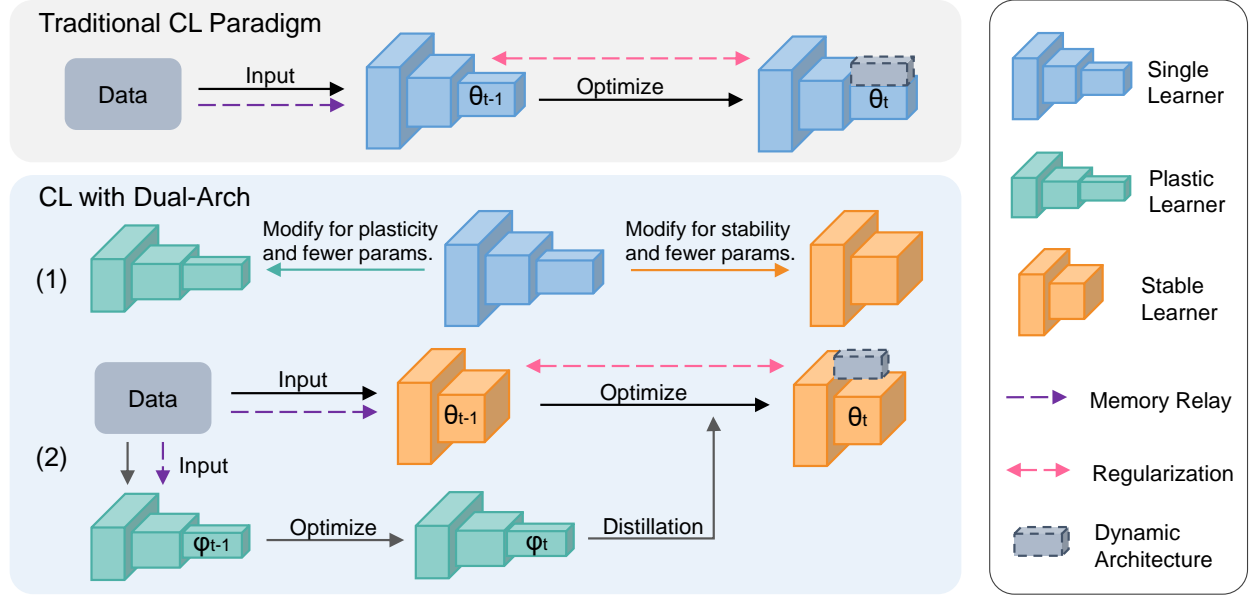


Figure 2: The formulation of the traditional CL paradigm and CL with Dual-Arch (Ours). Dual-Arch (1) employs two independent learners that are designed by modifying the traditional single learner, and (2) utilizes the stable learner to perform CL with the assistance of the plastic learner. Note that Dual-Arch can be effortlessly combined with existing CL methods (denoted by the dotted lines or box).

4.2. The Formulation of Dual-Arch

The overall framework of Dual-Arch is illustrated in Fig. 2. Unlike the existing CL paradigm which relies on a single learner, the Dual-Arch framework distributes the roles of plasticity and stability across two distinct models: the plastic learner and the stable learner. Inspired by existing research (Kim et al., 2023) that employs auxiliary models to enhance plasticity, our framework designates the stable learner as the main model, with the plasticity learner serving as an auxiliary model. Throughout the learning process, the plastic learner is dedicated to the extraction of new knowledge, allowing for the potential forgetting of previous knowledge. Conversely, the stable learner is responsible for retaining existing knowledge while integrating new knowledge with the assistance of the plastic learner.

Dual-Arch allows the combination of the strengths of both stable and plastic architectures by employing corresponding architectures for the two learners. Specifically, these architectures are designed through targeted modifications to the original one, with the objective of enhancing plasticity or stability. Additionally, to overcome the increased memory consumption associated with incorporating an additional model, we concurrently reduce the parameter counts for both learners. It is also worth highlighting that the Dual-Arch framework is designed to facilitate integration with a variety of CL methods, serving as a plug-and-play component. This integration can be easily achieved by applying these CL methods when training the stable learner, mir-

roring the training process of the single learner within the traditional CL paradigm. In particular, for replay-based methods, the replay buffer is concatenated with the training data for both the stable and plastic learners.

4.3. Architectures for the Stable and Plastic Learners

This subsection presents the specific architectural designs tailored to the stable and plastic learners, with the objective of achieving superior CL performance while minimizing parameter counts. Building upon the insights from Sec. 3, we employ a wide and shallow architecture for the stable learner, denoted as Sta-Net, and a deep and thin architecture for the plastic learner, denoted as Pla-Net. Following standard practices (Masana et al., 2022; Goswami et al., 2024), we have chosen ResNet-18 as the foundation for crafting both architectures. Specifically, Sta-Net retains the same width as ResNet-18 but incorporates only half as many residual blocks. Furthermore, we modify the GAP layer of Sta-Net to produce an output feature map of size 2×2 instead of the original 1×1 , thereby increasing the width of the classifier. To design Pla-Net, we maintain the depth of ResNet-18 while reducing its width from 64 to 42 to align with the parameter count of Sta-Net.

4.4. Learning Algorithm of Dual-Arch

The learning process of the Dual-Arch framework involves training the plastic and stable learners in sequence. In the

initial stage of the learning process, our framework trains the plastic learner as a new task emerges. At this stage, the primary objective is to facilitate the acquisition of new knowledge, without consideration of the maintenance of previously acquired knowledge. Consequently, the training objective of the plastic learner is simplified to minimize the classification loss on the current training data, i.e., $L_{plastic} = L_{CE}$. Subsequently, the stable learner is trained to integrate the existing knowledge with that acquired by the plastic learner. This process entails the transfer of recently acquired knowledge from the plastic learner to the stable learner via knowledge distillation. Specifically, a distillation loss term is incorporated into the training objective of the stable learner, to align the logit outputs between the stable and plastic learners. Following convention (Hinton et al., 2015), a hard label loss (i.e., cross-entropy loss) is also employed to minimize the discrepancy between the predictions of the stable learner and the actual labels of the training data. Moreover, established CL methods are implemented during this phase to facilitate the retention of previous knowledge, which can also be expressed as a loss term. In light of the aforementioned considerations, the total learning target of the stable learner can be formulated as:

$$L_{stable} = \alpha L_{CE} + (1 - \alpha) L_{KD} + L_{CL}, \quad (3)$$

where L_{KD} denotes the distillation loss and α is a parameter that balances the weight of L_{KD} and L_{CE} . We set the default value of α to 0.5, following (Hinton et al., 2015).

Within Dual-Arch, the distillation loss L_{KD} is employed to enhance the plasticity of the stable learner, which involves enabling it to learn from the soft outputs of the plastic learner. Specifically, the L_{KD} is calculated by measuring the Kullback-Leibler divergence between the soft outputs of the teacher model (i.e., the plastic learner) and those of the student model (the stable learner) on the current data. Let T denote the teacher model, and S denote the student model, the L_{KD} is defined as:

$$L_{KD} = - \sum_{i=1}^{N^k} P_T^i \log P_S^i, \quad (4)$$

where P_T and P_S represent the soft outputs of the teacher and student models. These soft outputs are derived by applying the SoftMax function to transform the output logits of these models, i.e., O_T and O_S , into probability distributions. Specifically, $P_T = \text{SoftMax}(O_T/t)$ and $P_S = \text{SoftMax}(O_S/t)$, where t is the temperature factor that controls the smoothness of the soft outputs.

The detailed training procedure of the proposed framework is summarized in Alg. 1. For each task k , the plastic learner is first trained to convergence using the standard classification loss L_{CE} . Its optimized weights are then frozen and preserved as a teacher model. Subsequently, the stable

learner is trained using the composite loss L_{stable} (Eq. 3), which incorporates knowledge from the teacher model. After each task, the stable learner is evaluated on all learned tasks (1 to k) to assess its CL performance.

Algorithm 1 Training Procedure of Dual-Arch

- 1: **Input:** Stable learner weights θ_0 , Plastic learner weights ϕ_0
 - 2: **Output:** Optimized stable learner weights θ_K
 - 3: **for** task $k = 1, 2, \dots, K$ **do**
 - 4: Train ϕ_{k-1} for E epochs using normal classification loss L_{CE} on task k to obtain ϕ_k
 - 5: Freeze ϕ_k and save as teacher model
 - 6: Train θ_{k-1} for E epochs using L_{stable} (Eq. (3)) on task k to obtain θ_k
 - 7: Evaluate θ_k on tasks (1 to k)
 - 8: **end for**
-

5. Experiment

5.1. Experiment Setup

Benchmark. Following convention (Rebuffi et al., 2017), We choose CIFAR100 (Krizhevsky et al., 2009) and ImageNet100 (Deng et al., 2009) for evaluation. Both datasets are divided into **10** tasks of 10 classes each and **20** tasks of 5 classes each to construct four benchmarks: CIFAR100/10, CIFAR100/20, ImageNet100/10, and ImageNet100/20.

Baselines. To assess the efficacy of our proposed method, we integrate it into five distinct CL approaches spanning the three major categories: replay-based, regularization-based, and architecture-based methods. These methods include iCaRL (Rebuffi et al., 2017), WA (Zhao et al., 2020), DER (Yan et al., 2021), Foster (Wang et al., 2022), and MEMO (Zhou et al., 2023b). Specifically, we compare the performance of Dual-Arch with that of the original ResNet-18 to evaluate the enhancements provided by our method. We also select ArchCraft (Lu et al., 2024) as a baseline, which employs a single CL-friendly architecture to improve CL performance, to show the benefits of dual architectures.

Implementation Setup. For all experiments, we train all models for 200 epochs in the first task and 100 epochs in the subsequent tasks. The learning rate starts from 0.1 and gradually decays with a cosine annealing scheduler. A fixed memory size of 2,000 exemplars is utilized for all replay-based methods during the learning process. Given the significant impact of hyper-parameters on CL (Cha & Cho, 2024; Mirzadeh et al., 2020), the hyperparameters for all methods adhere to the settings in the open-source library PyCIL (Zhou et al., 2023a) to ensure a fair comparison. Following convention (Mirzadeh et al., 2022b; Zhou et al., 2023a), the first convolution layer and following max pooling layer of networks are replaced by a 3×3 convolution

Table 2: The LA, AIA and FAF (%) using five state-of-the-art CL methods. ‘#P’ represents the parameter counts of all used models. ‘Improvement’ represents the boost of Dual-Arch towards original methods. Note that the parameter counts of DER and MEMO vary from incremental settings, resulting in two values for ‘/20’ and ‘/10’. **Bolded** indicates best.

Method	#P (M)	CIFAR100/20			CIFAR100/10			ImageNet100/20			ImageNet100/10		
		LA↑	AIA↑	FAF↓	LA↑	AIA↑	FAF↓	LA↑	AIA↑	FAF↓	LA↑	AIA↑	FAF↓
iCaRL	22.4	49.78	65.63	33.33	54.87	68.30	27.76	46.22	63.89	41.05	51.74	68.47	35.91
w/ ArchCraft	17.4	52.60	68.71	-	55.52	69.62	-	45.12	63.98	-	52.46	68.42	-
w/ Ours	15.1	52.53	67.80	29.49	57.69	70.40	23.63	47.22	65.06	35.66	54.84	69.37	28.22
Improvement	↓ 33%	+2.75	+2.17	↓3.84	+2.82	+2.10	↓4.13	+1.00	+1.17	↓5.39	+3.10	+0.90	↓7.69
WA	22.4	46.78	62.75	19.05	56.98	69.16	23.53	46.98	65.76	39.05	57.64	71.20	28.27
w/ ArchCraft	17.4	53.23	69.19	-	59.79	71.40	-	49.94	67.20	-	58.86	71.56	-
w/ Ours	15.1	55.02	68.84	24.91	59.78	71.57	17.91	52.84	68.79	31.73	60.84	72.57	24.53
Improvement	↓ 33%	+8.24	+6.09	↑5.86	+2.80	+2.41	↓5.62	+5.86	+3.03	↓7.32	+3.20	+1.37	↓3.74
DER	224.4/112.2	58.39	70.19	25.63	61.83	72.48	22.13	64.32	74.91	20.51	67.40	75.93	15.22
w/ ArchCraft	173.5/86.8	61.65	73.59	-	63.94	74.84	-	63.98	74.50	-	68.34	77.26	-
w/ Ours	106.9/55.9	64.08	73.86	20.08	66.22	75.08	17.73	65.40	75.17	16.97	68.52	77.49	12.96
Improvement	↓ 52%/50%	+5.69	+3.67	↓5.55	+4.39	+2.60	↓4.40	+1.08	+0.26	↓3.54	+1.12	+1.56	↓2.26
Foster	22.5	49.99	63.39	35.03	58.67	69.95	27.39	54.74	66.77	34.67	62.88	71.09	25.18
w/ ArchCraft	17.5	57.22	69.99	-	61.44	72.54	-	54.32	66.41	-	61.94	71.16	-
w/ Ours	15.4	57.69	71.01	23.75	61.23	73.22	18.23	55.20	67.63	32.42	63.24	72.42	25.04
Improvement	↓ 32%	+7.70	+7.62	↓11.28	+2.56	+3.27	↓9.16	+0.46	+0.86	↓2.25	+0.36	+1.33	↓0.14
MEMO	171.7/87.2	52.10	67.60	35.71	58.46	70.71	27.99	56.10	69.13	29.64	61.64	73.31	21.87
w/ ArchCraft	126.6/64.6	57.28	72.07	-	61.93	73.30	-	57.46	70.54	-	62.46	74.01	-
w/ Ours	101.1/53.1	62.39	72.69	24.09	65.35	74.34	20.82	60.26	72.53	24.59	65.40	75.54	16.53
Improvement	↓ 41%/39%	+10.29	+5.09	↓11.62	+6.89	+3.63	↓7.17	+4.16	+3.40	↓5.05	+3.76	+2.23	↓5.34

layer with a stride of 1 for CIFAR100.

Evaluation Metrics. The overall performance of CL is measured by two metrics: the *Last Accuracy* (LA) and the *Average Incremental Accuracy* (AIA). The LA is the total classification accuracy after the last task, which reflects the overall accuracy among all classes. Further, the AIA denotes the average classification accuracy over all tasks, which reflects the performance across all incremental steps. The higher LA and AIA, the better overall CL performance. Let K be the number of tasks, these two metrics are defined as $LA = A_K$, $AIA = \frac{1}{K} \sum_{b=1}^K A_b$, where A_b represents classification accuracy measured on the test set that covers all tasks learned up to and including the b -th task. Additionally, we report the FAF to quantify catastrophic forgetting.

5.2. Overall Results

Tab. 2 presents the comparative performance of Dual-Arch using five state-of-the-art CL methods. The results demonstrate that across various methods, datasets, and incremental steps, the integration of Dual-Arch consistently outperforms the baseline that employs ResNet-18 as a single learner. In particular, adopting Dual-Arch leads to maximum improvements of 10.29% in LA and 7.62% in AIA, while simultaneously reducing the parameter counts by at least 33%.

Moreover, Dual-Arch outperforms Arch-Craft in most cases, underscoring the advantages of dual architectures over a single, CL-friendly architecture. In conclusion, Dual-Arch emerges as a valuable complement to existing CL methods, enhancing both effectiveness and efficiency.

5.3. Ablation Study

In this subsection, we present the results of our ablation study to show the significance of employing dual networks in conjunction with dedicated architectures. To simplify, we select the CIFAR-100/10 as a representative dataset and utilize AIA as the performance metric for our analysis.

As displayed in Tab. 3, we examine the effects of removing two pivotal components from our method. Specifically, we present the outcomes of employing only a Sta-Net to underscore the necessity of the dual-networks framework, along with results from using alternative architectures for the two learners, highlighting the importance of tailored designs. We observe from Tab. 3 that the absence of a plastic learner leads to a decrease in AIA by an average of 2.63%. Similarly, employing non-specialized architectures for two learners within Dual-Arch results in lower performance, with the AIA declining by an average of 1.74%, 0.65%, and 1.68%. These results clearly demonstrate the benefits of

Table 3: The ablation study results using five CL methods. We report the mean \pm std of 3 runs with different initializations. \dagger denotes performing CL with a single learner. **Bolded** indicates the best.

Stable Learner	Plastic Learner	AIA (%) on CIFAR100/10					Average
		iCaRL	WA	DER	Foster	MEMO	
Sta-Net	Pla-Net	70.21 \pm 0.19	71.53 \pm 0.13	75.26 \pm 0.20	73.18 \pm 0.04	74.44 \pm 0.07	72.92
Sta-Net	None †	66.69 \pm 0.10	69.33 \pm 0.17	72.47 \pm 0.07	70.84 \pm 0.24	72.11 \pm 0.27	70.29 (-2.63)
Pla-Net	Pla-Net	69.57 \pm 0.10	69.98 \pm 0.08	74.64 \pm 0.28	71.92 \pm 0.28	69.80 \pm 0.15	71.18 (-1.74)
Sta-Net	Sta-Net	69.27 \pm 0.26	71.38 \pm 0.25	74.30 \pm 0.08	72.65 \pm 0.11	73.77 \pm 0.05	72.27 (-0.65)
Pla-Net	Sta-Net	69.85 \pm 0.13	70.31 \pm 0.26	74.25 \pm 0.35	71.86 \pm 0.06	69.92 \pm 0.12	71.24 (-1.68)

each component in our proposed solution.

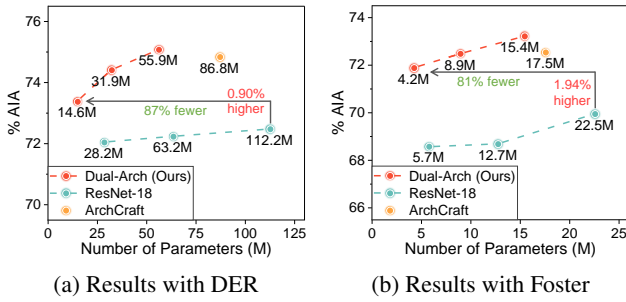


Figure 3: **Performance of CL vs. Number of Parameters** using DER and Foster on CIFAR100/10.

5.4. Parameter Efficiency Analysis

To assess the parameter efficiency more comprehensively, we vary the parameter counts of Dual-Arch and ResNet-18 by reducing the network width by a quarter and a half. As illustrated in Fig. 3, the Dual-Arch series significantly outperforms the baseline in terms of parameter efficiency. Specifically, Dual-Arch can enhance AIA by 0.90% and 1.94% when using DER and Foster as the CL method, respectively, while simultaneously reducing parameter counts by 87% and 81%. Additionally, Dual-Arch surpasses ArchCraft, a state-of-the-art solution that enhances parameter efficiency in CL by recrafting the network architecture. These empirical results highlight the potential of Dual-Arch to significantly benefit CL in memory-restricted scenarios.

5.5. Computation Efficiency Analysis

We note that although Dual-Arch involves training two models, the total computational cost, measured in FLOPs, remains lower than that of the baselines. For instance, on CIFAR-100, the FLOPs for Sta-Net and Pla-Net are 255M and 241M, respectively, yielding a combined total of 496M. In comparison, ResNet-18 requires approximately 558M FLOPs. Furthermore, during inference, only the stable learner is utilized, enabling Dual-Arch to achieve computa-

tional efficiency at test time (255M vs. 558M).

However, despite the reduced FLOPs, the training time increases due to the non-parallelizable nature of training the two learners. As illustrated in Table 4, Dual-Arch incurs a 1.39 \times to 1.77 \times overhead in training time compared to the baselines. This represents a limitation of our approach.

Table 4: Training time (minutes) comparison between Dual-Arch and baselines on CIFAR-100/10.

Method	iCaRL	WA	DER	Foster	MEMO
Original (ResNet-18)	40	39	74	93	49
w/ Dual-Arch (Ours)	70	69	106	129	85

5.6. Analysis on the Stability-Plasticity Trade-off

To further scrutinize the effectiveness of Dual-Arch in combining the strength of both architectures, we compare it to a single learner with one of the architectures (i.e., Pla-Net or Sta-Net). To simplify, we choose the top-performing approach DER as the used CL method. We observe from Fig. 4 (a) that Dual-Arch achieves the best overall performance in CL. Moreover, as illustrated in Fig. 4 (b) and (c), the single learner either forgets severely on previous tasks (Pla-Net) or underperforms on new ones (Sta-Net), whereas Dual-Arch demonstrates competitive performance in both aspects. This result indicates that Dual-Arch combines the advantages of both types of architecture, leading to a trade-off between stability and plasticity at the architectural level.

5.7. Analysis on Bias-correction

In *Class IL*, the task-recency bias is a major cause of catastrophic forgetting, where models tend to misclassify instances from earlier tasks as belonging to more recently introduced classes during inference (Masana et al., 2022; Zhao et al., 2020). To discover the reasons why Dual-Arch benefits CL, we further evaluate its effectiveness in mitigating the task-recency bias. Specifically, we present the task confusion matrices for the Dual-Arch and the baseline

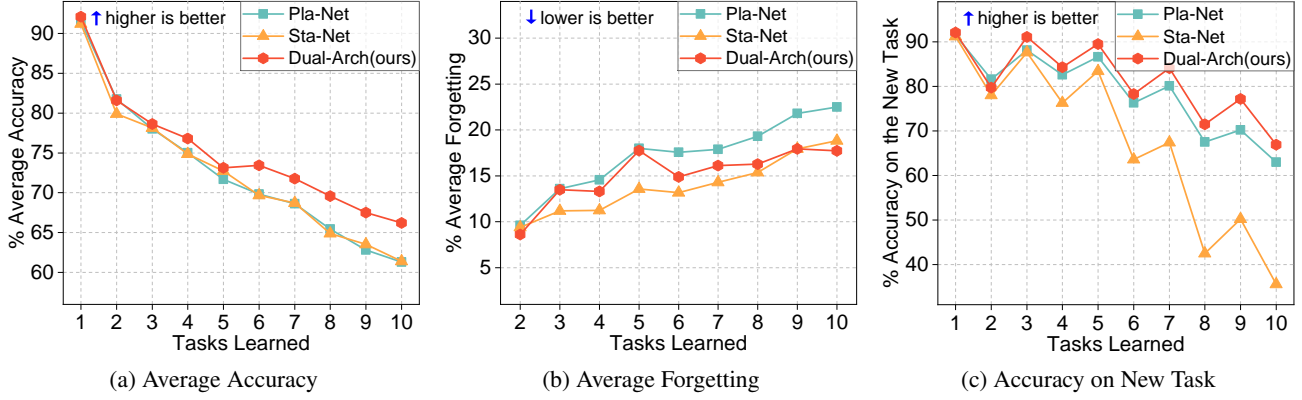


Figure 4: The performance of Dual-Arch and two baselines using DER on CIFAR100/10.

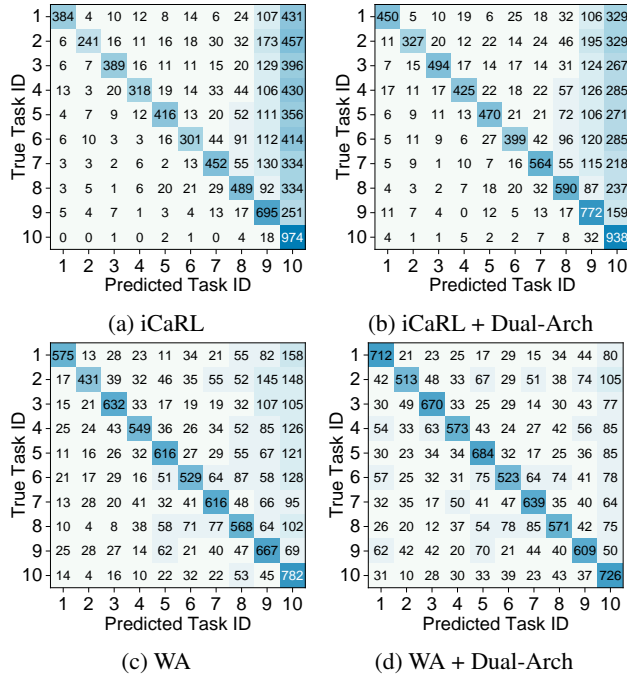


Figure 5: Task confusion matrices after learning the final task w/ and w/o Dual-Arch plugged in on CIFAR100/10.

which employs a single ResNet-18 in Fig. 5. From Fig. 5 (b) and (d), we observe that the integration of Dual-Arch facilitates a more precise determination of the correct task ID, thereby reducing inter-task classification errors. Notably, Dual-Arch significantly diminishes the misclassification of data from earlier tasks (e.g., task 1) as belonging to recently learned tasks (e.g., task 10). These observations indicate that Dual-Arch can effectively reduce the task-recency bias, thus mitigating catastrophic forgetting.

5.8. Validation on Vision Transformers

While our study primarily focuses on ResNet, the insights presented in this paper are potentially applicable to other

architectures, such as Vision Transformers (ViTs). To validate this, we conduct experiments to transfer our method to SepViT (Li et al., 2022), training all models from scratch and using ImageNet100/10 as the benchmark. It is important to note that the training settings remain consistent with those described in Sec. 5.1, with adjustments made to the learning rate and optimizer to align with the official implementation of SepViT (Li et al., 2022). The results, summarized in Tab. 5, demonstrate that Dual-Arch consistently improves the CL performance of SepViT, underscoring its potential generalizability to other architectures.

 Table 5: The LA and AIA (%) using SepViT on ImageNet100/10. ‘#P’ represents the parameter counts of all used networks. **Bolded** indicates the best.

Method	#P (M)	LA	AIA
iCaRL	7.57	43.08	60.62
w/ Ours	5.32	46.34 (+3.26)	63.09 (+2.47)
WA	7.57	38.40	57.67
w/ Ours	5.32	44.28 (+5.88)	61.15 (+3.48)

6. Conclusion

In this paper, we point out the stability-plasticity dilemma at the architectural level and further introduce Dual-Arch, a novel CL framework, to address it. Dual-Arch operates at an architectural level, complementary to most existing CL methods that focus on parameter optimization, thereby serving as a plug-in component for enhancing CL. Our extensive experiments demonstrate that Dual-Arch consistently outperforms the baselines while significantly reducing the parameter counts. We hope this work inspires further study on exploring a better trade-off between stability and plasticity from an architectural perspective.

Impact Statement

This paper presents work whose goal is to advance the field of Machine Learning. There are many potential societal consequences of our work, none which we feel must be specifically highlighted here.

Acknowledgement

This work was supported by National Natural Science Foundation of China under Grant 62276175 and Innovative Research Group Program of Natural Science Foundation of Sichuan Province under Grant 2024NSFTD0035.

References

- Aljundi, R., Lin, M., Goujaud, B., and Bengio, Y. Gradient based sample selection for online continual learning. *Advances in neural information processing systems*, 32, 2019.
- Arani, E., Sarfraz, F., and Zonooz, B. Learning fast, learning slow: A general continual learning method based on complementary learning system. In *International Conference on Learning Representations*, 2022.
- Bian, A., Li, W., Yuan, H., Wang, M., Zhao, Z., Lu, A., Ji, P., Feng, T., et al. Make continual learning stronger via c-flat. *NeurIPS*, 2024.
- Bonato, J., Pelosin, F., Sabetta, L., and Nicolosi, A. Mind: Multi-task incremental network distillation. In *Proceedings of the AAAI Conference on Artificial Intelligence*, volume 38, pp. 11105–11113, 2024.
- Buzzega, P., Boschini, M., Porrello, A., Abati, D., and Calderara, S. Dark experience for general continual learning: a strong, simple baseline. *Advances in neural information processing systems*, 33:15920–15930, 2020.
- Cha, S. and Cho, K. Hyperparameters in continual learning: a reality check. *arXiv preprint arXiv:2403.09066*, 2024.
- Chaudhry, A., Ranzato, M., Rohrbach, M., and Elhoseiny, M. Efficient lifelong learning with a-gem. *arXiv preprint arXiv:1812.00420*, 2018.
- Deng, J., Dong, W., Socher, R., Li, L.-J., Li, K., and Fei-Fei, L. Imagenet: A large-scale hierarchical image database. In *2009 IEEE conference on computer vision and pattern recognition*, pp. 248–255. Ieee, 2009.
- Feng, T., Wang, M., and Yuan, H. Overcoming catastrophic forgetting in incremental object detection via elastic response distillation. In *Proceedings of the IEEE/CVF Conference on Computer Vision and Pattern Recognition*, pp. 9427–9436, 2022.
- Feng, T., Li, W., Zhu, D., Yuan, H., Zheng, W., Zhang, D., and Tang, J. Zeroflow: Overcoming catastrophic forgetting is easier than you think. *arXiv preprint arXiv:2501.01045*, 2025.
- Goodfellow, I. J., Mirza, M., Xiao, D., Courville, A., and Bengio, Y. An empirical investigation of catastrophic forgetting in gradient-based neural networks. *arXiv preprint arXiv:1312.6211*, 2013.
- Goswami, D., Soutif-Cormerais, A., Liu, Y., Kamath, S., Twardowski, B., and van de Weijer, J. Resurrecting old classes with new data for exemplar-free continual learning. In *Proceedings of the IEEE/CVF Conference on Computer Vision and Pattern Recognition (CVPR)*, 2024.
- Gou, J., Yu, B., Maybank, S. J., and Tao, D. Knowledge distillation: A survey. *International Journal of Computer Vision*, 129(6):1789–1819, 2021.
- Grossberg, S. Adaptive resonance theory: How a brain learns to consciously attend, learn, and recognize a changing world. *Neural networks*, 37:1–47, 2013.
- He, K., Zhang, X., Ren, S., and Sun, J. Deep residual learning for image recognition. In *Proceedings of the IEEE conference on computer vision and pattern recognition*, pp. 770–778, 2016.
- Henning, C., Cervera, M., D’Angelo, F., Von Oswald, J., Traber, R., Ehret, B., Kobayashi, S., Grewe, B. F., and Sacramento, J. Posterior meta-replay for continual learning. *Advances in neural information processing systems*, 34:14135–14149, 2021.
- Hinton, G., Vinyals, O., and Dean, J. Distilling the knowledge in a neural network. *arXiv preprint arXiv:1503.02531*, 2015.
- Iscen, A., Zhang, J., Lazebnik, S., and Schmid, C. Memory-efficient incremental learning through feature adaptation. In *Computer Vision—ECCV 2020: 16th European Conference, Glasgow, UK, August 23–28, 2020, Proceedings, Part XVI 16*, pp. 699–715. Springer, 2020.
- Kim, S., Noci, L., Orvieto, A., and Hofmann, T. Achieving a better stability-plasticity trade-off via auxiliary networks in continual learning. In *Proceedings of the IEEE/CVF Conference on Computer Vision and Pattern Recognition*, pp. 11930–11939, 2023.
- Kirkpatrick, J., Pascanu, R., Rabinowitz, N., Veness, J., Desjardins, G., Rusu, A. A., Milan, K., Quan, J., Ramalho, T., Grabska-Barwinska, A., et al. Overcoming catastrophic forgetting in neural networks. *Proceedings of the national academy of sciences*, 114(13):3521–3526, 2017.

- Krizhevsky, A. et al. Learning multiple layers of features from tiny images. 2009.
- Kumaran, D., Hassabis, D., and McClelland, J. L. What learning systems do intelligent agents need? complementary learning systems theory updated. *Trends in cognitive sciences*, 20(7):512–534, 2016.
- Lee, H., Cho, H., Kim, H., Kim, D., Min, D., Choo, J., and Lyle, C. Slow and steady wins the race: Maintaining plasticity with hare and tortoise networks. In *International Conference on Machine Learning*, pp. 26416–26438. PMLR, 2024.
- Li, W., Wang, X., Xia, X., Wu, J., Li, J., Xiao, X., Zheng, M., and Wen, S. Sepvit: Separable vision transformer. *arXiv preprint arXiv:2203.15380*, 2022.
- Li, Z. and Hoiem, D. Learning without forgetting. *IEEE transactions on pattern analysis and machine intelligence*, 40(12):2935–2947, 2017.
- Liang, S. and Srikant, R. Why deep neural networks for function approximation? In *International Conference on Learning Representations*, 2017.
- Lu, A., Feng, T., Yuan, H., Song, X., and Sun, Y. Revisiting neural networks for continual learning: An architectural perspective. In *IJCAI*, pp. 4651–4659, 2024.
- Masana, M., Liu, X., Twardowski, B., Menta, M., Bagdanov, A. D., and Van De Weijer, J. Class-incremental learning: survey and performance evaluation on image classification. *IEEE Transactions on Pattern Analysis and Machine Intelligence*, 45(5):5513–5533, 2022.
- McClelland, J. L., McNaughton, B. L., and O’Reilly, R. C. Why there are complementary learning systems in the hippocampus and neocortex: insights from the successes and failures of connectionist models of learning and memory. *Psychological review*, 102(3):419, 1995.
- McCloskey, M. and Cohen, N. J. Catastrophic interference in connectionist networks: The sequential learning problem. In *Psychology of learning and motivation*, volume 24, pp. 109–165. Elsevier, 1989.
- Michel, N., Wang, M., Xiao, L., and Yamasaki, T. Rethinking momentum knowledge distillation in online continual learning. In *International Conference on Machine Learning*, pp. 35607–35622. PMLR, 2024.
- Mirzadeh, S. I., Farajtabar, M., Pascanu, R., and Ghasemzadeh, H. Understanding the role of training regimes in continual learning. *Advances in Neural Information Processing Systems*, 33:7308–7320, 2020.
- Mirzadeh, S. I., Chaudhry, A., Yin, D., Hu, H., Pascanu, R., Gorur, D., and Farajtabar, M. Wide neural networks forget less catastrophically. In *International Conference on Machine Learning*, pp. 15699–15717. PMLR, 2022a.
- Mirzadeh, S. I., Chaudhry, A., Yin, D., Nguyen, T., Pascanu, R., Gorur, D., and Farajtabar, M. Architecture matters in continual learning. *arXiv preprint arXiv:2202.00275*, 2022b.
- Pham, Q., Liu, C., and Hoi, S. Dualnet: Continual learning, fast and slow. *Advances in Neural Information Processing Systems*, 34:16131–16144, 2021.
- Pham, Q., Liu, C., and Steven, H. Continual normalization: Rethinking batch normalization for online continual learning. In *International Conference on Learning Representations*, 2022.
- Qin, H., Ding, Y., Zhang, X., Wang, J., Liu, X., and Lu, J. Diverse sample generation: Pushing the limit of generative data-free quantization. *TPAMI*, 2023.
- Raghu, M., Poole, B., Kleinberg, J., Ganguli, S., and Sohl-Dickstein, J. On the expressive power of deep neural networks. In *international conference on machine learning*, pp. 2847–2854. PMLR, 2017.
- Rebuffi, S.-A., Kolesnikov, A., Sperl, G., and Lampert, C. H. icarl: Incremental classifier and representation learning. In *Proceedings of the IEEE conference on Computer Vision and Pattern Recognition*, pp. 2001–2010, 2017.
- Robins, A. Catastrophic forgetting, rehearsal and pseudorehearsal. *Connection Science*, 7(2):123–146, 1995.
- Romero, A., Ballas, N., Kahou, S. E., Chassang, A., Gatta, C., and Bengio, Y. Fitnets: Hints for thin deep nets. *arXiv preprint arXiv:1412.6550*, 2014.
- Rosenfeld, A. and Tsotsos, J. K. Incremental learning through deep adaptation. *IEEE transactions on pattern analysis and machine intelligence*, 42(3):651–663, 2018.
- Rostami, M., Kolouri, S., and Pilly, P. K. Complementary learning for overcoming catastrophic forgetting using experience replay. In *Proceedings of the 28th International Joint Conference on Artificial Intelligence*, pp. 3339–3345, 2019.
- Rusu, A. A., Rabinowitz, N. C., Desjardins, G., Soyer, H., Kirkpatrick, J., Kavukcuoglu, K., Pascanu, R., and Hassabis, D. Progressive neural networks. *arXiv preprint arXiv:1606.04671*, 2016.
- Sarrafzadeh, F., Arani, E., and Zonooz, B. Synergy between synaptic consolidation and experience replay for general continual learning. In *Conference on Lifelong Learning Agents*, pp. 920–936. PMLR, 2022.

- Serra, J., Suris, D., Miron, M., and Karatzoglou, A. Overcoming catastrophic forgetting with hard attention to the task. In *International conference on machine learning*, pp. 4548–4557. PMLR, 2018.
- Simonyan, K. and Zisserman, A. Very deep convolutional networks for large-scale image recognition. *arXiv preprint arXiv:1409.1556*, 2014.
- Van de Ven, G. M., Tuytelaars, T., and Tolias, A. S. Three types of incremental learning. *Nature Machine Intelligence*, 4(12):1185–1197, 2022.
- Wang, F.-Y., Zhou, D.-W., Ye, H.-J., and Zhan, D.-C. Foster: Feature boosting and compression for class-incremental learning. In *European conference on computer vision*, pp. 398–414. Springer, 2022.
- Wang, F.-Y., Zhou, D.-W., Liu, L., Ye, H.-J., Bian, Y., Zhan, D.-C., and Zhao, P. Beef: Bi-compatible class-incremental learning via energy-based expansion and fusion. In *The Eleventh International Conference on Learning Representations*, 2023.
- Wang, L., Zhang, X., Su, H., and Zhu, J. A comprehensive survey of continual learning: Theory, method and application. *IEEE Transactions on Pattern Analysis and Machine Intelligence*, 2024a.
- Wang, M., Michel, N., Xiao, L., and Yamasaki, T. Improving plasticity in online continual learning via collaborative learning. In *Proceedings of the IEEE/CVF Conference on Computer Vision and Pattern Recognition*, pp. 23460–23469, 2024b.
- Yan, S., Xie, J., and He, X. Der: Dynamically expandable representation for class incremental learning. In *Proceedings of the IEEE/CVF conference on computer vision and pattern recognition*, pp. 3014–3023, 2021.
- Yoon, J., Yang, E., Lee, J., and Hwang, S. J. Lifelong learning with dynamically expandable networks. *arXiv preprint arXiv:1708.01547*, 2017.
- Zenke, F., Poole, B., and Ganguli, S. Continual learning through synaptic intelligence. In *International conference on machine learning*, pp. 3987–3995. PMLR, 2017.
- Zhao, B., Xiao, X., Gan, G., Zhang, B., and Xia, S.-T. Maintaining discrimination and fairness in class incremental learning. In *Proceedings of the IEEE/CVF conference on computer vision and pattern recognition*, pp. 13208–13217, 2020.
- Zhao, Z., Deng, L., Bai, H., Cui, Y., Zhang, Z., Zhang, Y., Qin, H., Chen, D., Zhang, J., Wang, P., and Gool, L. V. Image fusion via vision-language model. In *Proceedings of the International Conference on Machine Learning (ICML)*, 2024.
- Zhou, D.-W., Wang, F.-Y., Ye, H.-J., and Zhan, D.-C. Pycil: A python toolbox for class-incremental learning, 2023a.
- Zhou, D.-W., Wang, Q.-W., Ye, H.-J., and Zhan, D.-C. A model or 603 exemplars: Towards memory-efficient class-incremental learning. In *ICLR*, 2023b.

A. Appendix

A.1. Implementation Details

We employ the same data augmentation as in PyCIL (Zhou et al., 2023a) for all experiments. For the experiments in Section 3, we report results in different task orders using 5 seeds 1, 2, 3, 4, and 5. For other experiments, we adhere to a fixed seed of 1993, consistent with established conventions (Rebuffi et al., 2017; Zhou et al., 2023a). We utilize a temperature factor for Dual-Arch of $t = 4$ for CIFAR100 and $t = 3$ for ImageNet-100.

Details about Parameter Counts. We compute the sum of the parameter counts of all used models for each incremental step and report their peak values throughout the CL process as the final result. For instance, for iCaRL, we sum the parameter counts of the current and last models. For iCaRL with Dual-Arch, we sum the parameter counts of the plastic learner, the current stable learner, and the last stable learner. All results are detailed in Tab. 2 of the main paper. Moreover, it should be noted that the parameter counts vary slightly between the CIFAR100 and ImageNet100, and we report all results based on CIFAR100.

A.2. Architectural Dimensions of Stability and Plasticity in MLP

We further investigate the impact of network width (i.e., the number of neurons in the hidden layer) and depth (i.e., the number of layers) on the stability and plasticity of the MultiLayer Perceptron (MLP). Following HAT (Serra et al., 2018), we employ a width of 800 and a depth of 4 as the default design for the MLP. Additionally, we design a wider yet shallower variant and a deeper yet thinner variant, both with a parameter count comparable to the default design. We evaluated all MLPs on the split MNIST dataset, which consists of five tasks, using the LWF (Li & Hoiem, 2017). Note that we train all models with 10 epochs, and report results using five different task orders. The results are reported in Tab. 6. We observe that the wider yet shallower variant exhibits lower values for both AAN and FAF. These results suggest that within a fixed parameter budget, the wider and shallower variants offer superior stability at the expense of reduced plasticity, a trend consistent with the findings observed in ResNet architectures.

Table 6: The AAN and FAF (%) of MLP with different depths and widths. Note that the ‘#P’ denotes the parameter counts of a single architecture here.

Depth	Width	#P	AAN \uparrow	FAF \downarrow
4	800	1.92	84.20 \pm 5.37	42.10 \pm 7.58
3	1050	1.94	79.23 \pm 5.13 (-4.97)	26.78 \pm 5.18 (-15.32)
5	680	1.93	87.35 \pm 3.77 (+3.15)	59.28 \pm 6.71 (+17.18)

A.3. Architectural Dimensions of Stability and Plasticity in Vision Transformers

We further investigate the impact of network width (i.e., the dimension of the attention heads) and depth (i.e., the number of blocks) on the stability and plasticity of ViTs. Specifically, we use SepViT-Lite (Li et al., 2022) as the default design, which is configured with a width of 32 and a depth of 11. Additionally, we design a wider yet shallower variant with a width of 49 and depth of 5, which has a parameter count comparable to the default design. Both ViTs are evaluated on ImageNet-100/10 using iCaRL as the learning method (Rebuffi et al., 2017). Note that the training settings are consistent with Sec. 5.1, but the learning rate and optimizer are adjusted to match the official implementation of SepVit (Li et al., 2022). The results are reported in Tab. 7. We observe that the wider yet shallower variant exhibits lower values for both AAN and FAF. These results suggest that within a fixed parameter budget, the wider and shallower variants offer superior stability at the expense of reduced plasticity, a trend consistent with the findings observed in ResNet architectures.

Table 7: The AAN and FAF (%) of SepVit with different depths and widths. Note that the ‘#P’ denotes the parameter counts of a single architecture here.

Depth	Width	#P	AAN \uparrow	FAF \downarrow
11	32	3.78	79.54	40.51
5	49	3.76	78.96 (-0.58)	39.47 (-1.04)

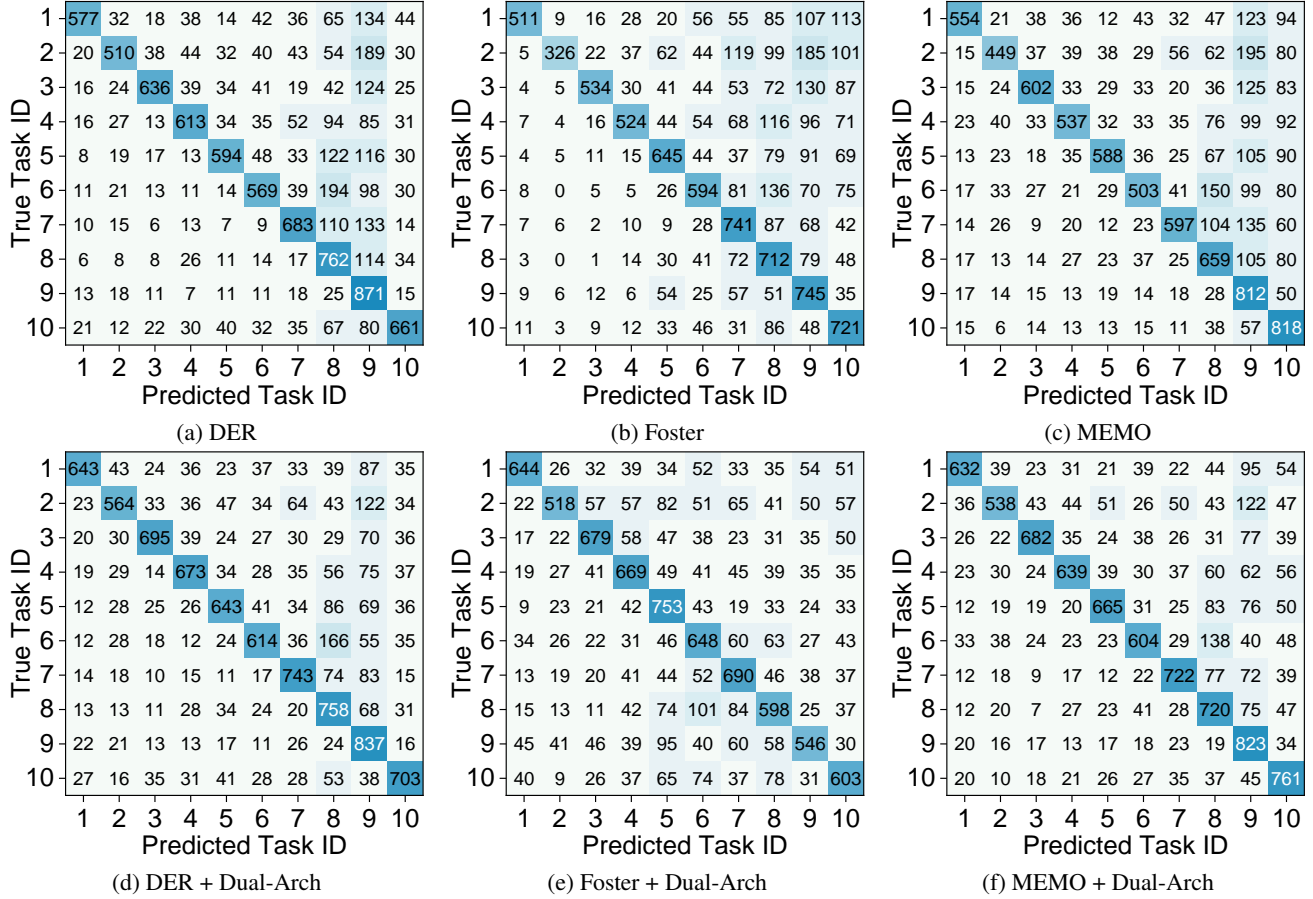


Figure 6: Task confusion matrices after learning the final task of different CL methods w/ and w/o Dual-Arch plugged in on CIFAR100/10.

A.4. Additional Results on Bias-correction

We report the task confusion matrices for the DER, Foster and MEMO with/without Dual-Arch here.

A.5. Validation on Long Task Sequences

In this subsection, we report the results on settings with a greater number of tasks, specifically CIFAR100/50, which contains 50 tasks, in Tab. 8. These results demonstrate that Dual-Arch consistently outperforms the baselines in this challenging setting, thereby underscoring its generality.

Table 8: The LA and AIA (%) using five state-of-the-art CL methods on CIFAR100/50. **Bolded** indicates the best.

Method	iCaRL		WA		DER		Foster		MEMO	
	LA	AIA	LA	AIA	LA	AIA	LA	AIA	LA	AIA
Original	45.30	63.99	42.12	58.26	55.73	69.53	43.45	59.81	42.44	62.57
w/ ArchCraft	48.70	67.24	39.83	61.02	57.89	71.53	53.02	68.14	54.47	69.96
w/ Ours	48.95	65.93	47.13	64.41	61.88	73.09	53.16	67.83	58.09	71.17

A.6. Validation on CL with Blurry Task Boundaries

Beyond Class-IL, a series of works have focused on a more challenging and realistic CL scenario where task boundaries are not explicitly available, known as Generalized Class IL (Buzzega et al., 2020; Arani et al., 2022). In this section, we validate the generality of Dual-Arch in this setting. Following convention (Arani et al., 2022; Sarfraz et al., 2022), we report the results on the typical benchmark, GCIL-CIFAR-100, as shown in Tab. 9. Our findings indicate that Dual-Arch consistently enhances CL performance in this scenario, underscoring its broad applicability.

Table 9: The LA (%) on GCIL-CIFAR-100 with different buffer sizes. **Bolded** indicates the best. Note that the benchmark settings follow (Arani et al., 2022).

Method	Buffer Size 500	Buffer Size 1000
ER (Rostami et al., 2019)	20.30	34.13
w/ Dual-Arch (Ours)	27.57 (+7.27)	35.40 (+1.27)
DER++ (Buzzega et al., 2020)	25.82	33.64
w/ Dual-Arch (Ours)	30.34 (+4.52)	36.84 (+3.20)